A Classical Interpretation of the Nonrelativistic Quark Potential Model: Color Charge Definition and the Meson Mass-Radius Relationship

ZhiGuang Tan,[1,*] YouNeng Guo,[1,†] ShengJie Wang,[1] and Hua Zheng[2,‡]

[1] *School of Electronic Information and Electrical Engineering, Changsha University,Changsha, 410003,P.R.China*
[2] *School of Physics and Information Technology, Shaanxi Normal University, Xi'an, 710119, China*

Quantum Chromodynamics (QCD) is the fundamental theory describing quark interactions, and various quark models based on QCD have been widely used to study the properties of hadrons, including their structures and mass spectra. However, unlike Quantum Electrodynamics (QED) and the Bohr model of the hydrogen atom, there is no direct classical analogy for hadronic structures. This paper presents a classical interpretation of the nonrelativistic quark potential model, providing a more intuitive and visualizable description of strong interactions through the quantitative formulation of color charge and color flux. Furthermore, we establish the relationship between meson mass and its radius in the nonrelativistic framework and estimate the key parameters of our model using available data from several heavy mesons. We then extend this relationship to a broader range of excited meson states, obtaining structural radii that show good agreement with the root mean square (RMS) radius or charge radius predicted by QCD calculations.

Keywords: Nonrelativistic Quark Potential Model; Color Charge; Color flux; Meson Structure; Mass spectra and radius

I. INTRODUCTION

When the Schrödinger equation

$$\nabla^2\Psi + \frac{2m}{\hbar^2}[E - V(r)]\Psi = 0 \tag{1}$$

is solved to obtain the eigenenergies and mass spectra of a meson system composed of a pair of positive and negative quarks, the potential function $V(r)$ of the system is pivotal, i.e., the so-called quark potential models [1–3]. Among them, the Cornell potential [4], proposed in the 1980s, has performed effectively. Most current potential models are based on it, incorporating various improvements or extensions [5, 6]. It is written as [4]

$$V(r) = -\frac{a}{r} + br, \tag{2}$$

where a and b are two positive parameters. The first term in Eq. (2) is the Coulomb-like potential, while the second term is to take into account the property of quark confinement. Thus, it is very difficult to separate a pair of attractive quarks. Solving Eq. (1) to obtain mass eigenstates and quantum properties of hadrons constitutes an approach to study the nature of those hadrons [7, 8]. In order to obtain results close to experimental measurements, not only can the parameters be adjusted, but the expression for the potential function can also be extended. In Refs. [9, 10], the potential has been extended to a more general form

$$V(r) = ar^2 + br - \frac{c}{r} + \frac{d}{r^2} + e. \tag{3}$$

However, except for the two terms as in Eq. (2), there are no physically reasonable explanations for the origins of the other terms in Eq. (3).

* tanzg@ccsu.edu.cn
† guoxuyan2007@163.com
‡ zhengh@snnu.edu.cn

According to a classical interpretation, the quantum numbers that describe the properties of hadrons [11] are inherently linked to their internal structure. So the interaction between quarks should be determined by their color charge values, relative positions, motion states and spin orientations. This study aims to identify the physical origins for each term in the potential model Eq. (3) and to provide a classical description of quark interactions.

The paper is organized as follows. In Sec. II, we introduce the concept of unit color charge and discuss the interaction between two stationary color charges in vacuum. We also provide the rule for the dot product of two color charges, along with the basic function, which corresponds to the Coulomb-like term in the potential Eq. (3). Section III explains the inverse square terms in the potential by introducing the concepts of color flow and color magnetic field. Section IV addresses the harmonic oscillator potential arising from spin, corresponding to the other three terms in Eq. (3). In Sec. V, we estimate the relevant model parameters and present our numerical results based on the classical description of meson structures, comparing them with data calculated from potential model in the literature. Finally, a brief summary and discussion are given in Sec. VI.

II. THE INTERACTION BETWEEN A PAIR OF STATIONARY QUARKS IN VACUUM

To provide a classical description of the interaction between a pair of quarks, we first define three fundamental color charges c_r, c_g, c_b and their corresponding anti-color charges $c_{\bar{r}}, c_{\bar{g}}, c_{\bar{b}}$ as follows

$$\begin{aligned} c_r &\equiv e^{\theta i}, \quad & c_{\bar{r}} &\equiv e^{\theta+\pi i} = -c_r; \\ c_g &\equiv e^{(\theta+\frac{2\pi}{3})i}, \quad & c_{\bar{g}} &\equiv e^{(\theta-\frac{\pi}{3})i} = -c_g; \\ c_b &\equiv e^{(\theta-\frac{2\pi}{3})i}, \quad & c_{\bar{b}} &\equiv e^{(\theta+\frac{\pi}{3})i} = -c_b; \end{aligned} \tag{4}$$

with $0 \le \theta < \pi$ in the complex plane. In fact, there is only a relative meaning between r, g and b. The modulus of each

color charge is 1, so it is also called the unit color charge. We can also represent them in the form of unit vectors in the unit circle, as shown in the Fig.1.

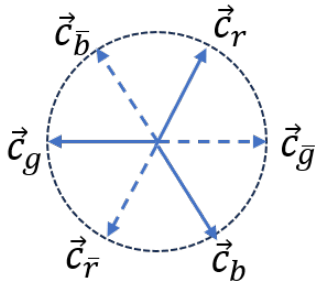

Fig. 1. Vector representation of unit color charge.

Obviously, they satisfy

$$c_i + c_{\bar{i}} = 0, \tag{5}$$

$$c_r + c_g + c_b = 0, \tag{6}$$

with $i = r, g, b$, ensuring the color neutrality of mesons and baryons. Color charges are quantized, which means that all color charges can only be integer mutiples of the three unit color charges aforementioned. The color charges can be added together as

$$C = \sum_{i=r,g,b} (n_i c_i + n_{\bar{i}} c_{\bar{i}}). \tag{7}$$

For example, a di-quark composed of a red color charge and a blue color charge results in an anti-green color charge. This allows the existence of particles with color charges other than unit color charges. The interaction between a pair of stationary color charges in vacuum is Coulomb-like which is defined as

$$\boldsymbol{F}_{C_1C_2} = Z\frac{C_1 \cdot C_2}{r^3}\boldsymbol{r}. \tag{8}$$

Here, Z is called the vacuum color gravitational constant and has units of Nm^2. The dot product between two unit color charges satisfies

$$c_i \cdot (\pm c_j) = \begin{cases} \pm 1, & i = j \\ \mp\frac{1}{2}, & i \neq j \end{cases} \qquad (i = r, g, b). \tag{9}$$

As shown in Fig. 2, one can verify that the total interaction between a blue quark (or antiquark) and a three quark cluster (with a total color charge of zero) is zero:

$$F = \sum_i^{r,g,b} Z\frac{\pm c_b \cdot c_i}{r^2} = Z\frac{\sum_i^{r,g,b} \pm c_b \cdot c_i}{r^2} = 0. \tag{10}$$

Obviously, when taking infinity as the zero point of color potential energy, the color potential energy between two color charges can be calculated by

$$E_p = \int_r^\infty \frac{F_{C_1C_2}}{r^2} dr = -Z\frac{C_1 \cdot C_2}{r}. \tag{11}$$

When $C_1 = -C_2$ and $|C_1| = 1$, the result above corresponds to the third term in Eq. (3)– the Coulomb-like term.

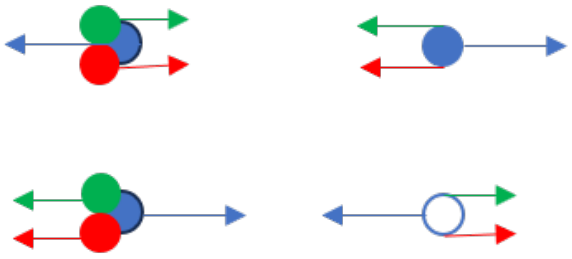

Fig. 2. The interaction between a blue quark(antiquark) and a three-quark cluster.

III. THE COLOR MAGNETIC FIELD FROM THE MOTION OF COLOR CHARGE

The collective motion of color charges generates color flow. Similarly to the electrical current intensity, the current intensity of color flow is defined as the amount of color charge flowing through a cross-section per unit time:

$$I_c = \frac{|\Delta C|}{\Delta t} = \frac{|\sum_{i=r}^{b}(n_i - n_{\bar{i}})c_i|}{\Delta t}. \tag{12}$$

It is assumed that color flow can generate a color magnetic field, modeled after Biot Savart's law:

$$\boldsymbol{B}_c = \int_l T\frac{I_c d\boldsymbol{l} \times \boldsymbol{r}}{r^3}. \tag{13}$$

Here, T is a parameter under vacuum, and its value needs to be measured directly or indirectly through experiments. For example, consider the color magnetic field generated by a circular color flow. As shown in Fig. 3, assuming the radius of the circular color current is a and the color current intensity is I_c, the following formulas can be derived by simulating the magnetic field generated by a circular current [12]

$$\begin{aligned} B_{cx} &= TI_c ar\cos\theta \int_0^{2\pi} \frac{\cos\varphi d\varphi}{(r^2 + a^2 - 2ra\sin\theta\cos\varphi)^{3/2}}, \\ B_{cy} &= 0, \\ B_{cz} &= TI_c \int_0^{2\pi} \frac{a^2 - ar\sin\theta\cos\varphi d\varphi}{(r^2 + a^2 - 2ra\sin\theta\cos\varphi)^{3/2}}. \end{aligned} \tag{14}$$

For points on the color flow plane, it is easy to see $\theta = \pi/2, \sin\theta = 1$, and $\cos\theta = 0$, therefore, $B_{cx} = B_{cy} = 0$, and

$$\begin{aligned} B_{cz} &= TI_c \int_0^{2\pi} \frac{a^2 - ar\cos\varphi d\varphi}{(r^2 + a^2 - 2ra\cos\varphi)^{3/2}} \\ &= 2TI_c \left[\frac{1}{a-r}E(k) + \frac{1}{a+r}K(k)\right] \\ &= 2TI_c X(a, r). \end{aligned} \tag{15}$$

Here, $E(k)$ and $K(k)$ are the elliptic functions ellipticE and ellipticK, respectively, with $k = 2\sqrt{ar}/(a + r)$. The color magnetic field diverges on the color flow circular line, as shown in Fig. 4.

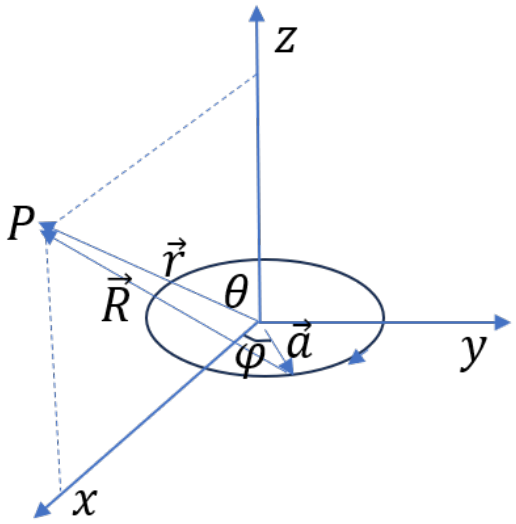

Fig. 3. The sketch of color magnetic field generated by a circular color flow.

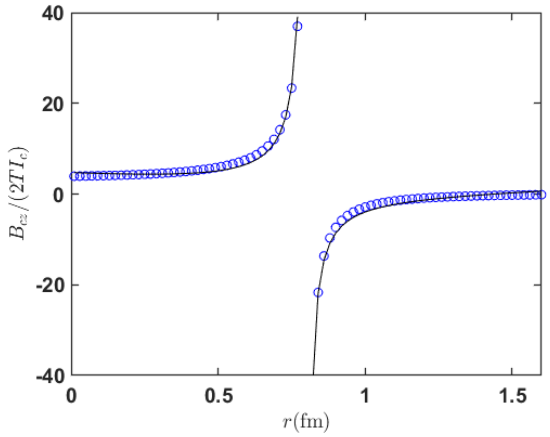

Fig. 4. The distribution of the color magnetic field generated by a circular color flow in the color flow plane. The small circles are calculated from Eq. (15), and the solid lines are the fits using Eq. (16).

For different radii of circular currents, we have obtained a simple explanatory formula for the inner and outer color magnetic fields of the circle through segmented fitting. Here, X_i and X_o represent the values of $B_{cz}/2TI_c$ inside and outside the circle, respectively.

$$
\begin{aligned}
a=0.5,\quad & X_i = 1.2215\frac{1}{a-r} + 9.9248(a-r),\\
& X_o = -0.8433\frac{1}{r-a} + 5.0440(r-a);\\
a=0.6,\quad & X_i = 1.2001\frac{1}{a-r} + 7.0576(a-r),\\
& X_o = -0.8593\frac{1}{r-a} + 3.6412(r-a);\\
a=0.7,\quad & X_i = 1.1833\frac{1}{a-r} + 5.2816(a-r),\\
& X_o = -0.8717\frac{1}{r-a} + 2.7549(r-a);\\
a=0.8,\quad & X_i = 1.1696\frac{1}{a-r} + 4.1042(a-r),\\
& X_o = -0.8817\frac{1}{r-a} + 2.1587(r-a);\\
a=0.9,\quad & X_i = 1.1583\frac{1}{a-r} + 3.2828(a-r),\\
& X_o = -0.8900\frac{1}{r-a} + 1.7381(r-a);\\
a=1.0,\quad & X_i = 1.1487\frac{1}{a-r} + 2.6866(a-r),\\
& X_o = -0.8970\frac{1}{r-a} + 1.4301(r-a).
\end{aligned}
\tag{16}
$$

The color magnetic field energy stored in a color flow ring can be calculated as follows:

$$E_{Bc} = \frac{1}{2}I_c\int \boldsymbol{B}_c\cdot d\boldsymbol{S} = TI_c^2\int_0^a X_i 2\pi r dr. \tag{17}$$

Since the value of T has not been determined yet, Fig. 5 shows the calculated values and the fitting relationship of $\frac{E_{Bc}}{TI_c^2}$ versus a, using Eq. (18)

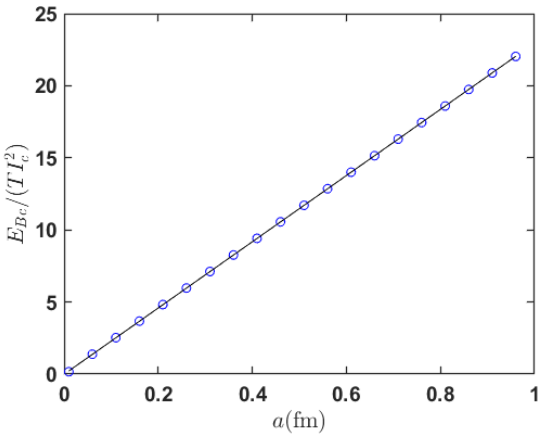

Fig. 5. The open circles are the results calculated by Eq. (17). The solid line is the fit using Eq. (18).

$$\frac{E_{Bc}}{TI_c^2} = 22.97a. \tag{18}$$

Now we can apply our scenario to mesons. When one quark orbits another quark in a circular motion with a radius r, its equivalent color flow intensity is

$$I_c = |c|\frac{v}{2\pi r} = \frac{v}{2\pi r}. \tag{19}$$

Taking into account the centripetal force provided by the color charge force,

$$Z\frac{1}{r^2} = m\frac{v^2}{r}, \tag{20}$$

the color magnetic energy stored in the meson is

$$E_{Bc} = 22.97TI_c^2 r = 0.5818T\frac{Z}{mr^2}. \tag{21}$$

This is the fourth term in the potential energy Eq. (3), which is inversely proportional to the square of the distance.

IV. THE HARMONIC OSCILLATOR POTENTIAL ORIGINATED FROM SPIN

In quantum mechanics, spin is an intrinsic property of particles. However, in classical terms, we propose that particle spin is an external manifestation of its internal structure. Here, we assume that the quark color charge undergoes circular motion around its own central axis, equivalent to a circular color flow ring, thereby possessing a colored magnetic moment. For a meson system composed of a pair of positive and negative quarks, as shown in Fig. 6, the color magnetic moments of the two quarks must be coplanar due to the effect of the chromomagnetic torque. Consequently, their spin orientations can only have two states: parallel or antiparallel. During their respective rotations, when the directions of the two color flows are parallel, the spin interaction is attractive. When the directions are antiparallel, the spin interaction is repulsive. If the color flow directions are perpendicular to each other, no force acts between them.

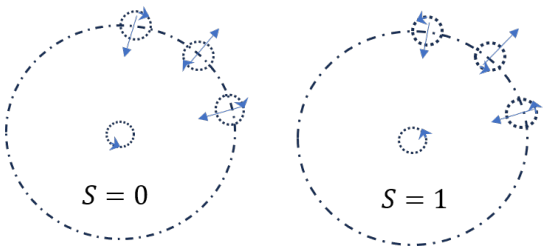

Fig. 6. Schematic diagram of spin interaction. When the color flow is parallel, they are attracted to each other. When it is antiparallel, they are repelled.

Therefore, spin induced interactions can be described by a harmonic oscillator, whose dynamic equilibrium position lies along the circumference of quark's orbital motion:

$$F_{S_1S_2} = -k(r' - r) = -\frac{1}{2}m\omega^2(r' - r). \tag{22}$$

Here, k is the elastic coefficient, and ω is the angular frequency. The total energy of the oscillator is

$$E_s = \frac{1}{2}kA^2 = \frac{1}{2}k(r_m - r)^2. \tag{23}$$

Expanding the right hand side of the above equation yields the remaining three terms of Eq. (3). Due to the extremely small size of $r_m - r$ (comparable to the radius of quarks), the vibrational energy is expressed using the quantum mechanical harmonic oscillator energy formula:

$$E_s = (L + \frac{1}{2})\hbar\omega_{nL}, \quad (L = 0, 1, 2, \cdots, n-1). \tag{24}$$

The top row in Fig. 7 represents the state where two quarks have the parallel spins, while the bottom row represents the state with antiparallel spins, i.e. $S_1 + S_2 = 0, 1$. Clearly, the stationary orbital motion period must satisfy a specific relationship with the spin period. As shown in Fig. 7, for a meson system to be in a stable state, the period of quark circular motion $T_\theta = 2\pi r/v$ must be an odd (for $S = 0$) or even(for $S = 1$) multiple of the vibration half-period, i.e.,

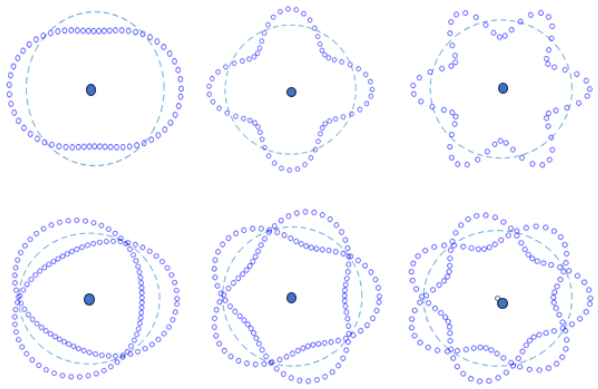

Fig. 7. Meson mechanics structure diagram with $n = 1, 2, 3$ from left to right. The top row corresponds to $S = 0$, while the bottom row is for $S = 1$.

$$\frac{2\pi r_{nL}}{v_{nL}} = \begin{cases} (2n-1)\frac{\pi}{\omega_{nL}}, & (S=0) \\ 2n\frac{\pi}{\omega_{nL}}, & (S=1) \end{cases} \quad n = 1, 2, \cdots \tag{25}$$

According to Eq. (20), one can obtain

$$r_{nL}^3 = \begin{cases} (n - \frac{1}{2})^2\frac{Z}{m\omega_{nL}^2}, & (S=0) \\ n^2\frac{Z}{m\omega_{nL}^2}, & (S=1) \end{cases} \tag{26}$$

Note that the terms ω_{nL} here do not represent the angular velocity of orbital motion, i.e., $\omega_{nL} \neq v_{nL}/r_{nL}$.

V. THE VALUES OF Z AND T AND RESULTS

Due to color confinement, it is impossible to directly measure the values of Z and T by measuring the forces between

two free quarks or two color currents. Instead, We can estimate their values using the masses and radii of certain hadrons measured experimentally.

In the center of mass frame of a meson, the mass of the meson can be calculated as [13, 14]

$$M_{nL} = M_Q + M_{\bar{q}} + E_{nL}. \tag{27}$$

Here, E_{nL} includes the previously mentioned E_p, E_{Bc}, E_s, and the kinetic energy $E_k = \frac{1}{2}mv^2 = \frac{Z}{2r}$, where the reduced mass is given by

$$m = \frac{M_Q M_{\bar{q}}}{M_Q + M_{\bar{q}}}. \tag{28}$$

Therefore, for a meson in a state with quantum number n and L, the classical calculation of its mass can be expressed as

$$\begin{aligned} M_{nL} &= M_Q + M_{\bar{q}} - \frac{Z}{2r_{nL}} + 0.5818T\frac{Z}{mr_{nL}^2} \\ &+ (L+\frac{1}{2})(n-\frac{1}{2}\delta_{S0})\sqrt{\frac{Z}{mr_{nL}^3}}. \end{aligned} \tag{29}$$

For the ground state radius r_{10} and mass M_{10} , we have

$$r_{10}^3 = \frac{Z\hbar^3}{4m\omega_{10}^2} \text{ or } \frac{Z\hbar^3}{m\omega_{10}^2}, \tag{30}$$

$$M_{10} = M - \frac{Z\hbar}{2r_{10}} + 0.5818T\frac{Z\hbar^2}{mr_{10}^2} + \frac{1}{2}\sqrt{\frac{\frac{1}{4}(1)Z\hbar^3}{mr_{10}^3}}, \tag{31}$$

where the natural unit $\hbar = 0.197$ GeV·fm=1 has been used. The values of Z and T are universal. This allows us to use a small amount of experimental data to deduce their values. Then, we use them to calculate the results for other mesons and test our model by the experimental data.

It is important to note that the previous discussion did not consider relativistic effects, which may require corrections for light meson systems. For heavy mesons, the relativistic effects are likely less significant, so we use heavy meson data to determine the values of Z and T.

Unfortunately, due to current experimental limitations, directly measuring meson radii is very challenging. However, model calculations of meson sizes have garnered significant interest among scientists. Currently, two important radii are used to describe the size of meson systems: the so-called root mean square (r.m.s.) radius $\langle r_{rms}^2\rangle$ [15, 16] and the charge radius $\langle r_E^2\rangle$ [17]. Their definitions are as follows:

$$\langle r_{rms}^2\rangle = \int_0^\infty r^2[\psi(r)]^2 dr, \tag{32}$$

$$\langle r_E^2\rangle = -6\frac{d^2}{dQ^2}eF(Q^2)|_{Q^2=0}, \tag{33}$$

where $\psi(r)$ is the radial wave function and $F(Q^2)$ is the form factor of the meson [18, 19]. According to calculations in Refs. [20, 21], the root mean square radius of the $\Upsilon(1S)$ state is approximately 0.2671 fm. Ref. [22], through a comprehensive contact interaction analysis, determined that the ground state charge radius of the pseudoscalar meson η_b is about 0.07 fm.

We use the data of these two mesons to determine the parameters Z and T. The mass data of these mesons are obtained from the Particle Data Group (PDG), while the mass of the constituent b quark is taken as $m_b = 4.95$ GeV, consistent with Refs. [20, 21]. These data are listed in TABLE 1. The obtained values of Z and T are

$n^{2S+1}L_j$	Name	$q\bar{q}'$	$\sqrt{\langle r_1\rangle^2}$ (fm)	M(GeV)
1^1S_0	$\eta_b(1S)$	$b\bar{b}$	0.070	9.3987
1^3S_1	$\Upsilon(1S)$	$b\bar{b}$	0.268	9.4604

TABLE 1. Meson data taken from PDG [27] and Refs. [20, 22].

$$Z = 9.46, \quad T = 0.615. \tag{34}$$

Convert to the International System of Units

$$Z = 2.98\times10^{-25}Nm^2, \quad T = 1.13\times10^{-43}Ns^2. \tag{35}$$

Comparing the magnitude of the gravitational forces between a pair of quark and antiquark that are 1 fm apart (with mass and charge of $m_b = m_{\bar{b}} = 4.95$ GeV, $q_b = -q_{\bar{b}} = -1/3e$)

$$F_m = G\frac{m_b m_{\bar{b}}}{r^2} = 5.16\times10^{-33}N, \tag{36}$$

$$F_e = k\frac{q_b q_{\bar{b}}}{r^2} = 2.56\times10N, \tag{37}$$

$$F_c = Z\frac{c_i c_{\bar{i}}}{r^2} = 8.17\times10^4N, \tag{38}$$

it is found that the strong interaction, based on color charge, is much greater than the other two, consistent with the hiearchy of forces magnitudes known. We use the meson masses provided by the Particle Data Group (PDG) [27] as inputs. By applying Eq. (29), we can calculate the corresponding meson radii and compare them with the results from other models, as shown in TABLE 2.

From TABLE 2, one can see that some of results are in good agreement with the results in the literature. It must be noted that existing literature on meson radius calculations employs various models [20, 22, 24, 28, 29], each with its own set of parameters, and most focus only on the lowest few states. Our model also relies on data from a few mesons; however, this is due to the current inability to experimentally measure Z and T. Once these two values are scientifically determined, a predictable relationship between meson mass and its structural radius can be established. As shown in Fig. 8, we present the mass-radius relationship for several quantum states of $b\bar{b}$ mesons using Eq. (29), which is of significant importance for understanding hadron structures.

VI. SUMMARY

In this article, we propose a classical interpretation based on color charge interactions for a pair of quarks. Specifically,

name	$q\bar{q}'$	state	$M(GeV)$	ω	$r_{nL}(fm)$	$\sqrt{r^2}$[Ref.]
$\eta_b(1S)$	$b\bar{b}$	1^1S_0	9.3987	0.9093	0.0700	0.07[22]
$\Upsilon(1S)$	$b\bar{b}$	1^3S_1	9.4604	0.8352	0.2680	0.2671[22]
$\chi_{b0}(1P)$	$b\bar{b}$	1^3P_0	9.8594	0.2972	0.4340	0.39[22]
$\chi_{b1}(1P)$	$b\bar{b}$	1^3P_1	9.8928	0.3586	0.3830	
$h_b(1P)$	$b\bar{b}$	1^1P_1	9.8993	0.3694	0.3755	
$\chi_{b2}(1P)$	$b\bar{b}$	1^3P_2	9.9122	0.3910	0.3615	
$\Upsilon(2S)$	$b\bar{b}$	2^3S_1	10.0233	2.3623	0.1730	
$\Upsilon_2(1D)$	$b\bar{b}$	1^3D_2	10.1637	0.3019	0.4295	
$\chi_{b0}(2P)$	$b\bar{b}$	2^3P_0	10.2325	0.5209	0.4740	
$\chi_{b1}(2P)$	$b\bar{b}$	2^3P_1	10.2555	0.5448	0.4600	
$h_b(2P)$	$b\bar{b}$	2^1P_1	10.2598	0.6445	0.3395	
$\chi_{b2}(2P)$	$b\bar{b}$	2^3P_2	10.2687	0.5575	0.4530	
$\Upsilon(3S)$	$b\bar{b}$	3^3S_1	10.3552	2.7877	0.2030	
$\chi_{b1}(3P)$	$b\bar{b}$	3^3P_1	10.5134	0.6839	0.5180	
$\chi_{b2}(3P)$	$b\bar{b}$	3^3P_2	10.5240	0.6939	0.5130	
$\Upsilon(4S)$	$b\bar{b}$	4^3S_1	10.5794	3.0422	0.2320	
$\Upsilon(5S)$	$b\bar{b}$	5^3S_1	10.8761	3.5696	0.2420	
$\eta_c(1S)$	$c\bar{c}$	1^1S_0	2.9839	0.7948	0.2090	0.20[22]
$J/\psi(1S)$	$c\bar{c}$	1^3S_1	3.0969	0.9675	0.2910	0.37[23]
						0.28[24]
$\chi_{c0}(1P)$	$c\bar{c}$	1^3P_0	3.4147	0.4539	0.4820	0.43[22]
$\chi_{c1}(1P)$	$c\bar{c}$	1^3P_1	3.5107	0.5368	0.4310	
$h_c(1P)$	$c\bar{c}$	1^1P_1	3.5254	0.6262	0.2450	
$\chi_{c2}(1P)$	$c\bar{c}$	1^3P_2	3.5662	0.5839	0.4075	
$\eta_c(2S)$	$c\bar{c}$	2^1S_0	3.6375	2.1065	0.2270	0.386[24]
$\psi(2S)$	$c\bar{c}$	2^3S_1	3.6861	2.1773	0.2690	0.387[24]
$\psi(3770)$	$c\bar{c}$	$2^3P_{0,1}$	3.7737	0.6569	0.5980	
$\psi_2(3823)$	$c\bar{c}$	2^3P_2	3.8237	0.6967	0.5750	
$\psi_3(3842)$	$c\bar{c}$	2^3P_3	3.8427	0.7715	0.5670	
$\chi_{c1}(3872)$	$c\bar{c}$	2^3P_1	3.8717	0.7347	0.5550	
$\chi_{c0}(3915)$	$c\bar{c}$	2^1P_0	3.9217	0.8122	0.4285	
$\chi_{c2}(3930)$	$c\bar{c}$	2^3P_2	3.9225	0.7741	0.5360	
B_c^+	$c\bar{b}$	1^1S_0	6.2745	0.0920	0.7650	0.38 ∼
						1.09[25]
$B_c^+(2S)$	$c\bar{b}$	2^1S_0	6.8712	0.2290	0.1900	0.17[22]
B_s^0	$s\bar{b}$	1^1S_0	5.3669	0.4514	0.3680	0.24[22]
B_s^*	$s\bar{b}$	1^3S_1	5.5154	0.7485	0.4170	
$B_{s1}(5830)^0$	$s\bar{b}$	1^3P_1	5.8286	0.4359	0.5980	
$B_{s2}^*(5840)^0$	$s\bar{b}$	1^3P_2	5.8399	0.4448	0.5900	
D^+	$c\bar{d}$	1^1S_0	5.2793	2.5089	0.1370	0.10 ∼
						0.42 [26]
D^0	$c\bar{u}$	1^1S_0	1.8648	0.3175	0.5435	0.14 ∼
						0.55[26]
D_s^+	$c\bar{s}$	1^1S_0	1.9683	0.3607	0.4535	0.10 ∼
						0.4[26]
η'	$s\bar{s}$	1^1S_0	0.9578	0.2934	0.5990	0.5[26]

TABLE 2. The results of our model for the particles in PDG. The last column contains reference values from the literature.

the design of the superposition and dot product of quark color charges predicts the existence of non unit color charge elementary particles. Analogous to electromagnetic fields, we introduce the concepts of color flow, color field, and color magnetic field. Model parameters Z and T are estimated using known data of few heavy mesons. The effectiveness of our model has been validated by comparing our results with literature data, which show good agreement. However, the precise calculation of the energy spectrum structure of

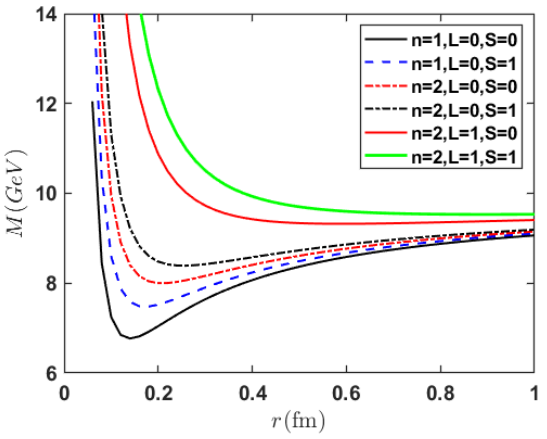

Fig. 8. The relationship between the mass and radius of a heavy meson composed of a bottom quark (b) and an anti-bottom quark ($\bar{b}$) using Eq. (29).

hadrons relies on Quantum Chromodynamics. We expect that the classical approach presented in this article provides a simple and visualizable method to study the interior of microscopic particles, analogous to Bohr model of the hydrogen atom in quantum mechanics.

ACKNOWLEDGMENTS

This work was supported in part by the Department of Education (grant No. 21A0541) and Natural Science Foundation (grant No.2025JJ50382) of Hunan province, China.

[1] C. Semay, B. Silvestre-Brac, Potential models and meson spectra. Nucl. Phys. A **618**, 455 (1997). https://doi.org/10.1016/S0375-9474(97)00060-2

[2] K. Watanabe, Quark-diquark potential and diquark mass from lattice QCD. Phys. Rev. D **105**, 074510 (2022). https://doi.org/10.1103/PhysRevD.105.074510

[3] Z. Zhao, K. Xu, A. Limphirat et al., Mass spectrum of 1^{--} heavy quarkonium. Phys. Rev. D **109**, 016012 (2024). https://doi.org/10.1103/PhysRevD.109.016012

[4] E. Eichten, K. Gottfried, T. Kinoshita et al., Charmonium: comparison with experiment. Phys. Rev. D **21**, 203 (1980). https://doi.org/10.1103/PhysRevD.21.203

[5] A.I. Ahmadov, K.H. Abasova, M.S. Orucova, Bound state solution schrödinger equation for extended cornell potential at finite temperature. Advances in High Energy Physics **2021**, 1861946 (2021). https://doi.org/10.1155/2021/1861946

[6] L.P. Fulcher, Z. Chen, K.C. Yeong, Energies of quark-antiquark systems, the Cornell potential, and the spinless Salpeter equation. Phys. Rev. D **47**, 4122 (1993). https://doi.org/10.1103/PhysRevD.47.4122

[7] F.X. Liu, R.H. Ni, X.H. Zhong et al., Charmed-strange tetraquarks and their decays in the potential quark model. Phys. Rev. D **107**, 096020 (2023). https://doi.org/10.1103/PhysRevD.107.096020

[8] T.Y. Li, L. Tang, Z.Y. Fang et al., Higher states of the B_c meson family. Phys. Rev. D **108**, 034019 (2023). https://doi.org/10.1103/PhysRevD.108.034019

[9] V. Kumar, R.M. Singh, S.B. Bhardwaj et al., Analytical solutions to the Schrödinger equation for a generalized Cornell potential and its applications to diatomic molecules and heavy mesons. Mod. Phys. Lett. A **37**, 2250010 (2022). https://doi.org/10.1142/S0217732322500109

[10] M. Abu-Shady, E.M. Khokha, Bound state solutions of the Dirac equation for the generalized Cornell potential model. Int. J. Mod. Phys. A **36**, 2150195 (2021). https://doi.org/10.1142/S0217751X21501955

[11] Z.G. Tan, S.J. Wang, Y.N. Guo et al., A novel encoding mechanism for particle physics. Nucl. Sci. Tech. **35**, 144 (2024). https://doi.org/10.1007/s41365-024-01537-8

[12] J.M. Griffith, G.W. Pan, Time harmonic fields produced by circular current loops. IEEE transactions on magnetics **47**, 2029 (2011). https://doi.org/10.1109/TMAG.2011.2132731

[13] M. Abu-Shady, T.A. Abdel-Karim, S. Y. Ezz-Alarab, Masses and thermodynamic properties of heavy mesons in the non-relativistic quark model using the Nikiforov-Uvarov method. J. Egyptian Math. Soc. **27**, 14 (2019). https://doi.org/10.1186/s42787-019-0014-0

[14] R. Rani, S.B. Bhardwaj, F. Chand, Mass spectra of heavy and light mesons using asymptotic iteration method. Commun. Theor. Phys. **70**, 179 (2018). https://doi.org/10.1088/0253-6102/70/2/179

[15] N. Akbar, B. Masud, S. Noor, Wave-function-based characteristics of hybrid mesons. Eur. Phys. J. A **47**, 124 (2011). https://doi.org/10.1140/epja/i2011-11124-2

[16] A.M. Yasser, G.S. Hassan, T.A. Nahool, A study of some properties of bottomonium. Journal of Modern Physics **5**, 1938 (2014). http://dx.doi.org/10.4236/jmp.2014.517188

[17] K.U. Can, G. Erkol, M. Oka et al., Vector and axial-vector couplings of D and D^* mesons in 2+1 flavor lattice QCD. Phys. Lett. B **719**, 103 (2013). https://doi.org/10.1016/j.physletb.2012.12.050

[18] D.P. Stanley, D. Robson, Nonperturbative potential model for light and heavy quark-antiquark systems. Phys. Rev. D **21**, 3180 (1980). https://doi.org/10.1103/PhysRevD.21.3180

[19] H.T. Ding, X. Gao, A.D. Hanlon et al., QCD Predictions for Meson Electromagnetic Form Factors at High Momenta: Testing Factorization in Exclusive Processes. Phys. Rev. Lett. **133**, 181902 (2024). https://doi.org/10.1103/PhysRevLett.133.181902

[20] C.W. Hwang. Charge radii of light and heavy mesons, Eur. Phys. J. C **23**, 585 (2002). https://doi.org/10.1007/s100520200904

[21] T. Das, Treatment of N-dimensional Schrö dinger equation for anharmonic potential via Laplace transform. arXiv:1408.6139. https://doi.org/10.48550/arXiv.1408.6139

[22] R.J. Hernández-Pinto, L.X. Gutiérrez-Guerrero, A. Bashir et al., Electromagnetic form factors and charge radii of pseudoscalar and scalar mesons: A comprehensive contact interaction analysis. Phys. Rev. D **107**, 054002 (2023). https://doi.org/10.1103/PhysRevD.107.054002

[23] D. Ebert, R.N. Faustov, V.O. Galkin, Spectroscopy and Regge trajectories of heavy quarkonia and B_c mesons. Eur. Phys. J. C **71**, 1825 (2011). https://doi.org/10.1140/epjc/s10052-011-1825-9

[24] L. Adhikari, Y. Li, M. Li et al., Form factors and generalized parton distributions of heavy quarkonia in basis light front quantization. Phys. Rev. C **99**, 035208 (2019). https://doi.org/10.1103/PhysRevC.99.035208

[25] T. Das, D.K. Choudhury, K.K. Pathak, RMS and charge radii in a potential model. Indian J. Phys. **90**, 1307 (2016). https://doi.org/10.1007/s12648-016-0866-1

[26] T. Das, K.K. Pathak, D.K. Choudhury, Three-Loop Effect in rms and Charge Radii of Heavy Flavored Mesons in a QCD Potential Model. Int. J. Theor. Phys. **63**, 172 (2024). https://doi.org/10.1007/s10773-024-05697-6

[27] (Particle Data Group) C. Patrignani, K. Agashe, G. Aielli et al., Review of Particle Physics. Chin. Phys. C **40**, 100001 (2016). https://iopscience.iop.org/article/10.1088/1674-1137/40/10/100001

[28] A. Höll, A. Krassnigg, P. Maris et al., Electromagnetic properties of ground-state and excited-state pseudoscalar mesons. Phys. Rev. C **71**, 065204 (2005). https://doi.org/10.1103/PhysRevC.71.065204

[29] A.F. Krutov, R.G. Polezhaev, V.E. Troitsky, Radius of the ρ meson determined from its decay constant. Phys. Rev. D **93**, 036007 (2016). https://doi.org/10.1103/PhysRevD.93.036007